GUIDED DYNAMIC POSITIONING FOR FULLY ACTUATED MARINE SURFACE VESSELS

Morten Breivik[1,3] **Jann Peter Strand**[2] **Thor I. Fossen**[1]

Abstract: This paper addresses the topic of dynamic positioning (DP) for fully actuated marine surface vessels. The concept of guided DP is developed by employing a modular motion control design procedure. In any DP application, the main objective is to track a planar target point while attaining a certain vessel heading. As such, this work considers both the case where the target point moves along a fully known path, as well as the case where only instantaneous target point information is available.

Keywords: Guided dynamic positioning, Fully actuated vessels, Modular design concept

1. INTRODUCTION

The concept of dynamic positioning (DP) was originally conceived in the 1960s, when drillships in the offshore oil and gas industry had to be positioned at locations where it was impossible to deploy conventional anchors due to large water depths. Hence, DP entails that surface vessels maintain their position exclusively by means of active propulsors and thrusters. Traditionally, DP-capable vessels have mainly been found within the offshore segment of the marine industries, with applications including deep-water drilling, diving support, pipelaying, anchor handling, and (heavy-lift) crane operations. However, recent years has seen an upsurge of vessels that serve other marine segments also acquire DP capabilities. Examples include passenger and cargo vessels, research and survey vessels, as well as naval vessels. Today, DP applications encompass not only station keeping, but also low-speed maneuvering operations. A basic overview of a DP system can be found in (Holvik 1998), while (Bray 2003) thoroughly treats all practical aspects related to DP of surface vessels.

The first DP-capable vessels that appeared at the beginning of the 1960s were controlled manually, but were soon retrofitted with analogue controllers for increased operational precision through automatic control. Subsequently, due to significant advances within digital computer technology, digitally implemented controllers rapidly replaced their analogue counterparts. These early controllers were based on the classical proportional-integral-derivative (PID) principle, controlling each of the 3 horizontal degrees of freedom (DOFs) independently. In the 1970s, more sophisticated linear controllers based on optimal control theory were introduced, steadily enhanced through the 1980s (Sælid *et al.* 1983) and 1990s (Sørensen *et al.* 1996) by the introduction of new state estimation and wave filtering techniques. However, linear controllers can only ensure local stability properties, so inspired by work performed in the field of robotics, nonlinear control theory was utilized in the late 1990s to guarantee global stability results (Fossen 2002).

The main focus concerning DP technology is related to practical aspects such as control allocation, power management, and signal processing. Less attention has been paid to the fundamental and underlying principles of motion control associated with the DP controllers, resulting for instance in the fact that state-of-the-art implementations are not readily extendable to handle underactuated vessels. Consequently, the focus and main contribution of this paper is a motion control concept named *guided dynamic positioning*, which is inspired by theory from both path following

[1] {Centre for Ships and Ocean Structures, Department of Engineering Cybernetics}, Norwegian University of Science and Technology (NTNU), NO-7491 Trondheim, Norway. E-mails: {morten.breivik, fossen}@ieee.org.

[2] Rolls-Royce Marine AS, P.O. Box 826, NO-6001 Aalesund, Norway. E-mail: jann_peter.strand@rolls-royce.com.

[3] Supported by the Research Council of Norway through the Centre for Ships and Ocean Structures at NTNU.

and missile guidance. This concept not only entails helmsman-like motion behavior, but also straightforward extension toward underactuated operations.

2. GUIDED DYNAMIC POSITIONING

Here, the concept of guided dynamic positioning is developed by means of a backstepping-inspired and cascaded-based design procedure. The motion control scenario entails tracking a stationary or time-varying *target point* in the plane while attaining a desired vessel heading. The consideration involves both the case where the target point moves along a path that is fully known, as well as the case where only instantaneous information about the target point is available. Since this work only treats fundamental aspects, specific issues pertaining to control allocation, state estimation, or wave filtering are disregarded. However, standard solutions to such topics are readily applicable for fully actuated vessels that employ the proposed DP scheme. In what follows, the time derivative (of a vector) $\mathbf{x}(t)$ is denoted $\dot{\mathbf{x}}$, the partial derivative of $\mathbf{x}(\varpi(t))$ is denoted $\mathbf{x}'$ $\left(= \frac{\partial \mathbf{x}}{\partial \varpi}(\varpi(t))\right)$, while $|\cdot|$ represents the Euclidean vector norm and the induced matrix norm.

2.1 Dynamic Model of a Marine Surface Vessel

A 3 degree-of-freedom (DOF) dynamic model of the horizontal surge, sway, and yaw modes can be found in (Fossen 2002), and consists of the kinematics

$$\dot{\boldsymbol{\eta}} = \mathbf{R}(\psi)\boldsymbol{\nu}, \tag{1}$$

and the kinetics

$$\mathbf{M}\dot{\boldsymbol{\nu}} + \mathbf{C}(\boldsymbol{\nu})\boldsymbol{\nu} + \mathbf{D}(\boldsymbol{\nu})\boldsymbol{\nu} = \boldsymbol{\tau} + \mathbf{R}(\psi)^\top \mathbf{b}, \tag{2}$$

where $\boldsymbol{\eta} = [x, y, \psi]^\top \in \mathbb{R}^2 \times \mathcal{S}$ represents the earth-fixed position and heading (with $\mathcal{S} = [-\pi, \pi]$), $\boldsymbol{\nu} = [u, v, r]^\top \in \mathbb{R}^3$ represents the vessel-fixed velocity, $\mathbf{R}(\psi) \in SO(3)$ is the transformation matrix

$$\mathbf{R}(\psi) = \begin{bmatrix} \cos\psi & -\sin\psi & 0 \\ \sin\psi & \cos\psi & 0 \\ 0 & 0 & 1 \end{bmatrix} \tag{3}$$

that transforms from the vessel-fixed BODY frame (**B**) to the earth-fixed NED frame (**N**), $\mathbf{M}$ is the inertia matrix, $\mathbf{C}(\boldsymbol{\nu})$ is the centrifugal and coriolis matrix, while $\mathbf{D}(\boldsymbol{\nu})$ is the hydrodynamic damping matrix. The system matrices satisfy the properties $\mathbf{M} = \mathbf{M}^\top > 0$, $\mathbf{C} = -\mathbf{C}^\top$ and $\mathbf{D} > 0$. The vessel-fixed propulsion forces and moment is represented by $\boldsymbol{\tau} = [\tau_{\mathrm{X}}, \tau_{\mathrm{Y}}, \tau_{\mathrm{N}}]^\top \in \mathbb{R}^3$, corresponding to a fully actuated vessel. Full actuation means that all 3 DOFs can be independently controlled simultaneously, i.e., the direction of the linear velocity is independent of the heading of the vessel. This is not the case for an underactuated craft, where the orientation of the linear velocity is inherently coupled (in a sense locked) to the heading. Finally, $\mathbf{b}$ represents the low-frequency earth-fixed environmental forces that act on the vessel.

2.2 Motion Control Scenario

In our scenario, the dynamic positioning problem for a fully actuated marine surface vessel can be stated by

$$\lim_{t\to\infty} (\boldsymbol{\eta}(t) - \boldsymbol{\eta}_{\mathrm{d}}(t)) = \mathbf{0}, \tag{4}$$

where $\boldsymbol{\eta}_{\mathrm{d}}(t) = \left[\mathbf{p}_{\mathrm{t}}^\top(t), \psi_{\mathrm{d}}(t)\right]^\top \in \mathbb{R}^2 \times \mathcal{S}$ represents the earth-fixed position and heading associated with the target point. We consider both the case where $\mathbf{p}_{\mathrm{t}}(t)$ is stationary (i.e., point stabilization) and time-varying (i.e., trajectory tracking), while $\psi_{\mathrm{d}}(t)$ can be chosen arbitrarily (e.g., as an auxiliary task objective).

2.3 Motion Control Design

We now employ a backstepping-inspired and cascaded-based design approach to develop the concept of guided dynamic positioning, and consider both the case where the target point moves along a path that is fully known (Case A), as well as the case where only instantaneous information about the target point is available (Case B). Due to the modular nature of the suggested scheme, we first design a motion controller (control loop) by means of integrator backstepping. A key feature is that this controller applies to both case A and B, by feeding it with the respectively appropriate reference signals. These signals (guidance loop) are specifically designed for each case.

2.3.1. Control Loop Design Since the position of a vessel can be controlled through its linear velocity, we redefine the output space of the controller from the nominal 3 DOF position and heading to the 3 DOF linear velocity and heading (Fossen *et al.* 2003). Consequently, consider the positive definite and radially unbounded Control Lyapunov Function (CLF)

$$V_{\mathrm{g}} = \frac{1}{2}(z_\psi^2 + \mathbf{z}_\nu^\top \mathbf{M}\mathbf{z}_\nu + \tilde{\mathbf{b}}^\top \boldsymbol{\Gamma}^{-1}\tilde{\mathbf{b}}) \tag{5}$$

where we have

$$z_\psi = \psi - \psi_{\mathrm{d}} \tag{6}$$

and

$$\mathbf{z}_\nu = \boldsymbol{\nu} - \boldsymbol{\alpha}, \tag{7}$$

where $\boldsymbol{\alpha} = [\alpha_u, \alpha_v, \alpha_r]^\top \in \mathbb{R}^3$ is a so-called vector of stabilizing functions (virtual inputs that become reference signals) yet to be designed. Also,

$$\tilde{\mathbf{b}} = \hat{\mathbf{b}} - \mathbf{b} \tag{8}$$

represents an adaptation error where $\hat{\mathbf{b}}$ is the estimate of $\mathbf{b}$, and by assumption $\dot{\mathbf{b}} = \mathbf{0}$. Finally, $\boldsymbol{\Gamma} = \boldsymbol{\Gamma}^\top > 0$ is the so-called adaptation gain matrix.

Then, differentiate the CLF with respect to time to ultimately obtain the negative semi-definite

$$\dot{V}_{\mathrm{g}} = -k_\psi z_\psi^2 - \mathbf{z}_\nu^\top (\mathbf{D} + \mathbf{K}_\nu)\mathbf{z}_\nu \tag{9}$$

by choosing the virtual input $\mathbf{h}^\top \boldsymbol{\alpha} = \alpha_{\mathrm{r}}$ as

$$\alpha_{\mathrm{r}} = \dot{\psi}_{\mathrm{d}} - k_\psi z_\psi, \tag{10}$$

where $k_\psi > 0$ is a constant, and

$$\mathbf{h} = [0, 0, 1]^\top ; \tag{11}$$

by choosing the control input as

$$\boldsymbol{\tau} = \mathbf{M}\dot{\boldsymbol{\alpha}} + \mathbf{C}\boldsymbol{\alpha} + \mathbf{D}\boldsymbol{\alpha} - \mathbf{R}^\top \hat{\mathbf{b}} - \mathbf{h} z_\psi - \mathbf{K}_\nu \mathbf{z}_\nu \tag{12}$$

where $\mathbf{K}_\nu = \mathbf{K}_\nu^\top > 0$ is a constant matrix; and by choosing the disturbance adaptation update law as

$$\dot{\hat{\mathbf{b}}} = \boldsymbol{\Gamma}\mathbf{R}\mathbf{z}_\nu. \tag{13}$$

Considering the vector $\mathbf{z}_\mathrm{g} = \left[z_\psi, \mathbf{z}_\nu^\top, \tilde{\mathbf{b}}^\top\right]^\top$, we can now state the following fundamental proposition

Proposition 1. The equilibrium point $\mathbf{z}_\mathrm{g} = \mathbf{0}$ is rendered uniformly globally asymptotically and locally exponentially stable (UGAS/ULES) by adhering to (10), (12) and (13) under the assumption that $\boldsymbol{\alpha}$ and $\dot{\boldsymbol{\alpha}}$ are uniformly bounded.

PROOF. The proposed result follows by straightforward application of Theorem 1 in (Fossen *et al.* 2001).

It is interesting to note that this motion controller cannot achieve anything meaningful unless it is fed sensible reference signals, i.e., unless $\boldsymbol{\alpha}_\mathrm{v} = [\alpha_\mathrm{u}, \alpha_\mathrm{v}]^\top \in \mathbb{R}^2$ is purposefully defined. However, therein lies also its strength, i.e., its universal applicability; to achieve whatever the design of $\boldsymbol{\alpha}_\mathrm{v}$ implies. We now proceed to design the reference signals solving case A and B.

2.3.2. Case A: Tracking a Target Along a Path Here, we consider the case where the motion control designer is granted the freedom to design the path (trajectory) that is to be traversed, as well as the motion of a target point that is to be tracked along the path. The theory is taken from the path following part of (Breivik and Fossen 2006). Consequently, consider a (planar) path continuously parameterized by a scalar variable $\varpi \in \mathbb{R}$, such that the position of a point belonging to the path is represented by $\mathbf{p}_\mathrm{p}(\varpi) \in \mathbb{R}^2$. Thus, the path is a one-dimensional manifold expressible by the set

$$\mathcal{P} = \left\{\mathbf{p} \in \mathbb{R}^2 \mid \mathbf{p} = \mathbf{p}_\mathrm{p}(\varpi)\ \forall \varpi \in \mathbb{R}\right\}. \tag{14}$$

Then, consider a time-varying target point $\mathbf{p}_\mathrm{t}(t) = \mathbf{p}_\mathrm{p}(\varpi_\mathrm{t}(t))$ traversing the path by adhering to a chosen speed profile $U_\mathrm{t}(\varpi_\mathrm{t})$, implemented through

$$\dot{\varpi}_\mathrm{t} = \frac{U_\mathrm{t}(\varpi_\mathrm{t})}{\left|\mathbf{p}_\mathrm{p}'(\varpi_\mathrm{t})\right|}, \tag{15}$$

since $|\dot{\mathbf{p}}_\mathrm{t}| = \left|\mathbf{p}_\mathrm{p}'(\varpi_\mathrm{t})\right| \dot{\varpi}_\mathrm{t} = U_\mathrm{t}(\varpi_\mathrm{t})$, where $U_\mathrm{t}(\varpi_\mathrm{t}) \in [U_{\mathrm{t,min}}, U_{\mathrm{t,max}}]$, $U_{\mathrm{t,min}} > 0$.

2.3.2.1. Guidance Loop Design We now design the required *orientation* of $\boldsymbol{\alpha}_\mathrm{v}$ (given that $|\boldsymbol{\alpha}_\mathrm{v}| > 0$) such that a vessel controlled by (12) and (13) achieves path following. Consequently, consider the positive definite and radially unbounded CLF

$$V_\varepsilon = \frac{1}{2}\boldsymbol{\varepsilon}^\top \boldsymbol{\varepsilon}, \tag{16}$$

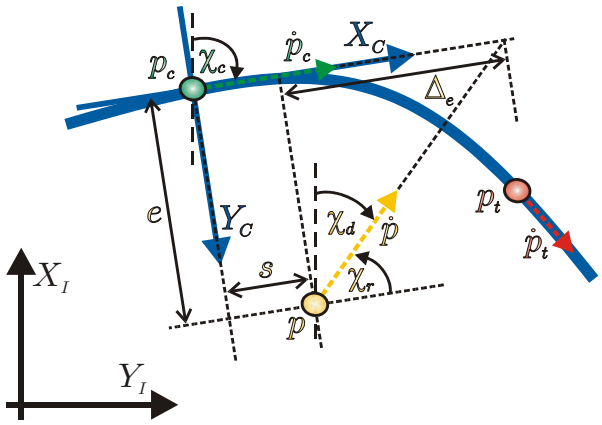

Fig. 1. The basic geometry behind tracking along a planar path. The vessel is shown in orange, the collaborator in green, and the target point in red.

with

$$\boldsymbol{\varepsilon} = \mathbf{R}_\mathrm{C}^\top (\mathbf{p} - \mathbf{p}_\mathrm{c}) \tag{17}$$

where $\mathbf{p}_\mathrm{c} = \mathbf{p}_\mathrm{p}(\varpi_\mathrm{c})$ represents a *collaborator* point that acts cooperatively with the marine craft as an intermediate path attractor, and whose sole purpose is to ensure that the vessel can converge to the path even if it has not converged to the target point. For a given ϖ_c, define a path-tangential reference frame at $\mathbf{p}_\mathrm{c}$ termed the COLLABORATOR frame (**C**). To arrive at **C**, the INERTIAL frame (**I**) must be positively rotated

$$\chi_\mathrm{c} = \arctan\left(\frac{y_\mathrm{p}'(\varpi_\mathrm{c})}{x_\mathrm{p}'(\varpi_\mathrm{c})}\right), \tag{18}$$

which can be represented by the rotation matrix

$$\mathbf{R}_\mathrm{C} = \begin{bmatrix} \cos\chi_\mathrm{c} & -\sin\chi_\mathrm{c} \\ \sin\chi_\mathrm{c} & \cos\chi_\mathrm{c} \end{bmatrix}, \tag{19}$$

$\mathbf{R}_\mathrm{C} \in SO(2)$. Hence, equation (17) represents the error vector between the vessel and its collaborator decomposed in **C**. The local coordinates $\boldsymbol{\varepsilon} = [s, e]^\top$ consist of the along-track error s and the cross-track error e. It is clear that path following can be achieved by driving $\boldsymbol{\varepsilon}$ to zero, see Figure 1. Thus, differentiate the CLF in (16) along the trajectories of $\boldsymbol{\varepsilon}$ to obtain

$$\begin{aligned}
\dot{V}_\varepsilon &= \boldsymbol{\varepsilon}^\top \dot{\boldsymbol{\varepsilon}} \\
&= \boldsymbol{\varepsilon}^\top (\mathbf{S}_\mathrm{C}^\top \mathbf{R}_\mathrm{C}^\top (\mathbf{p} - \mathbf{p}_\mathrm{c}) + \mathbf{R}_\mathrm{C}^\top (\dot{\mathbf{p}} - \dot{\mathbf{p}}_\mathrm{c})) \\
&= \boldsymbol{\varepsilon}^\top \left(\mathbf{S}_\mathrm{C}^\top \boldsymbol{\varepsilon} + \mathbf{R}_\mathrm{C}^\top \mathbf{H}\dot{\boldsymbol{\eta}} - \mathbf{v}_\mathrm{c}\right) \\
&= \boldsymbol{\varepsilon}^\top \left(\mathbf{R}_\mathrm{C}^\top \mathbf{H}\mathbf{R}\boldsymbol{\nu} - \mathbf{v}_\mathrm{c}\right)
\end{aligned}$$

where $\mathbf{S}_\mathrm{C} = -\mathbf{S}_\mathrm{C}^\top \Rightarrow \boldsymbol{\varepsilon}^\top \mathbf{S}_\mathrm{C}^\top \boldsymbol{\varepsilon} = 0$, and where

$$\mathbf{H} = \begin{bmatrix} 1 & 0 & 0 \\ 0 & 1 & 0 \end{bmatrix}. \tag{20}$$

Also, $\mathbf{v}_\mathrm{c} = [U_\mathrm{c}, 0]^\top$, where $U_\mathrm{c} = |\dot{\mathbf{p}}_\mathrm{c}|$, represents the linear velocity of the collaborator decomposed in **C**. Furthermore, we have that

$$\begin{aligned}
\dot{V}_\varepsilon &= \boldsymbol{\varepsilon}^\top \left(\mathbf{R}_\mathrm{C}^\top \mathbf{H}\mathbf{R}\boldsymbol{\alpha} - \mathbf{v}_\mathrm{c}\right) + \boldsymbol{\varepsilon}^\top \mathbf{R}_\mathrm{C}^\top \mathbf{H}\mathbf{R}\mathbf{z}_\nu \\
&= \boldsymbol{\varepsilon}^\top \left(\mathbf{R}_\mathrm{C}^\top \mathbf{H}\mathbf{R}\mathbf{H}^\top \mathbf{H}\boldsymbol{\alpha} - \mathbf{v}_\mathrm{c}\right) + \boldsymbol{\varepsilon}^\top \mathbf{R}_\mathrm{C}^\top \mathbf{H}\mathbf{R}\mathbf{H}^\top \mathbf{H}\mathbf{z}_\nu,
\end{aligned}$$

since $\boldsymbol{\nu} = \mathbf{z}_\nu + \boldsymbol{\alpha}$ and $\mathbf{H}^\top\mathbf{H} = \mathbf{I}_{3\times 3}$ (identity matrix). Defining $\mathbf{H}\mathbf{R}\mathbf{H}^\top = \mathbf{R}_\mathrm{B}$, i.e.,

$$\mathbf{R}_\mathrm{B} = \begin{bmatrix} \cos\psi & -\sin\psi \\ \sin\psi & \cos\psi \end{bmatrix}, \tag{21}$$

leads to

$$\dot{V}_\varepsilon = \boldsymbol{\varepsilon}^\top \left(\mathbf{R}_\mathrm{C}^\top \mathbf{R}_\mathrm{B}\mathbf{H}\boldsymbol{\alpha} - \mathbf{v}_\mathrm{c}\right) + \boldsymbol{\varepsilon}^\top \mathbf{R}_\mathrm{C}^\top \mathbf{R}_\mathrm{B}\mathbf{H}\mathbf{z}_\nu,$$

where $\mathbf{R}_\mathrm{B}\mathbf{H}\boldsymbol{\alpha} = \mathbf{R}_\mathrm{B}\boldsymbol{\alpha}_{\mathrm{v,B}}$ with $\boldsymbol{\alpha}_{\mathrm{v,B}} = \boldsymbol{\alpha}_\mathrm{v} = [\alpha_\mathrm{u}, \alpha_\mathrm{v}]^\top$. Now, $\mathbf{R}_\mathrm{B}\boldsymbol{\alpha}_{\mathrm{v,B}} = \mathbf{R}_\mathrm{DV}\boldsymbol{\alpha}_{\mathrm{v,DV}} = \boldsymbol{\alpha}_{\mathrm{v,I}}$ represents the desired linear velocity decomposed in **I**, while $\boldsymbol{\alpha}_{\mathrm{v,DV}} = [U_\mathrm{d}, 0]^\top$, where $U_\mathrm{d} = |\boldsymbol{\alpha}_\mathrm{v}|$, represents the desired linear velocity decomposed in a DESIRED VELOCITY frame (**DV**). This frame is aligned with $\boldsymbol{\alpha}_{\mathrm{v,I}}$, whose orientation we want to design so as to achieve path following. Hence, we get

$$\begin{aligned}\dot{V}_\varepsilon &= \boldsymbol{\varepsilon}^\top \left(\mathbf{R}_\mathrm{C}^\top \mathbf{R}_\mathrm{DV}\boldsymbol{\alpha}_{\mathrm{v,DV}} - \mathbf{v}_\mathrm{c}\right) + \boldsymbol{\varepsilon}^\top \mathbf{R}_\mathrm{C}^\top \mathbf{R}_\mathrm{B}\mathbf{H}\mathbf{z}_\nu \\ &= \boldsymbol{\varepsilon}^\top \left(\mathbf{R}_\mathrm{R}\boldsymbol{\alpha}_{\mathrm{v,DV}} - \mathbf{v}_\mathrm{c}\right) + \boldsymbol{\varepsilon}^\top \mathbf{R}_\mathrm{C}^\top \mathbf{R}_\mathrm{B}\mathbf{H}\mathbf{z}_\nu,\end{aligned}$$

where $\mathbf{R}_\mathrm{C}^\top(\chi_\mathrm{c})\mathbf{R}_\mathrm{DV}(\chi_\mathrm{d}) = \mathbf{R}_\mathrm{R}(\chi_\mathrm{d} - \chi_\mathrm{c})$, i.e., the relative orientation between **C** and **DV**.

Thus, U_c and $(\chi_\mathrm{d} - \chi_\mathrm{c})$ can be considered as virtual inputs for driving $\boldsymbol{\varepsilon}$ to zero, given that $U_\mathrm{d} > 0$. Denote the angular difference by $\chi_\mathrm{r} = \chi_\mathrm{d} - \chi_\mathrm{c}$, and expand the CLF derivative to obtain

$$\dot{V}_\varepsilon = s(U_\mathrm{d}\cos\chi_\mathrm{r} - U_\mathrm{c}) + eU_\mathrm{d}\sin\chi_\mathrm{r} + \boldsymbol{\varepsilon}^\top \mathbf{R}_\mathrm{C}^\top \mathbf{R}_\mathrm{B}\mathbf{H}\mathbf{z}_\nu,$$

where U_c can be chosen as

$$U_\mathrm{c} = U_\mathrm{d}\cos\chi_\mathrm{r} + \gamma s \tag{22}$$

with $\gamma > 0$ constant, while χ_r can be selected as

$$\chi_\mathrm{r} = \arctan\left(-\frac{e}{\triangle_\mathrm{e}}\right) \tag{23}$$

with $\triangle_\mathrm{e} > 0$ (not necessarily constant; a variable that is often referred to as a lookahead distance in literature treating planar path following along straight lines), giving

$$\dot{V}_\varepsilon = -\gamma s^2 - U_\mathrm{d}\frac{e^2}{\sqrt{e^2 + \triangle_\mathrm{e}^2}} + \boldsymbol{\varepsilon}^\top \mathbf{R}_\mathrm{C}^\top \mathbf{R}_\mathrm{B}\mathbf{H}\mathbf{z}_\nu. \tag{24}$$

Consequently

$$\dot{\varpi}_\mathrm{c} = \frac{U_\mathrm{c}}{|\mathbf{p}_\mathrm{c}'|} \tag{25}$$

and

$$\chi_\mathrm{d} = \chi_\mathrm{c} + \chi_\mathrm{r}, \tag{26}$$

with U_c as in (22), χ_c as in (18), and χ_r as in (23). Equations (25) and (26) indicate that the collaborator point continuously leads the vessel, while the desired linear velocity of the vessel must point at the path-tangential associated with the collaborator, in the direction of forward motion. Specifically, the desired linear velocity $\boldsymbol{\alpha}_\mathrm{v}$ must be computed by

$$\begin{aligned}\boldsymbol{\alpha}_\mathrm{v} &= \mathbf{R}_\mathrm{B}^\top \mathbf{R}_\mathrm{DV}\boldsymbol{\alpha}_{\mathrm{v,DV}} \\ &= \begin{bmatrix} U_\mathrm{d}\cos(\chi_\mathrm{d} - \psi) \\ U_\mathrm{d}\sin(\chi_\mathrm{d} - \psi) \end{bmatrix}.\end{aligned} \tag{27}$$

Then, write the system dynamics of $\boldsymbol{\varepsilon}$ and $\mathbf{z}_\mathrm{g}$ as

$$\Sigma_{\mathrm{A.1}} : \dot{\boldsymbol{\varepsilon}} = \mathbf{f}_{\mathrm{A.1}}(t, \boldsymbol{\varepsilon}) + \mathbf{g}_{\mathrm{A.1}}(t, \boldsymbol{\varepsilon}, \mathbf{z}_\mathrm{g})\mathbf{z}_\mathrm{g} \tag{28}$$

$$\Sigma_{\mathrm{A.2}} : \dot{\mathbf{z}}_\mathrm{g} = \mathbf{f}_{\mathrm{A.2}}(t, \mathbf{z}_\mathrm{g}), \tag{29}$$

which is a pure cascade where the control subsystem perturbs the guidance subsystem through the matrix

$$\mathbf{g}_{\mathrm{A.1}}(t, \boldsymbol{\varepsilon}, \mathbf{z}_\mathrm{g}) = \left[\mathbf{0}_{2\times 1}, \mathbf{R}_\mathrm{C}^\top \mathbf{R}_\mathrm{B}\mathbf{H}, \mathbf{0}_{2\times 3}\right]. \tag{30}$$

Also, consider the following assumptions

Assumption 2. $\left|\mathbf{p}_\mathrm{p}'\right| \in \left[\left|\mathbf{p}_\mathrm{p}'\right|_{\min}, \left|\mathbf{p}_\mathrm{p}'\right|_{\max}\right] \; \forall \varpi \in \mathbb{R}$

Assumption 3. $\triangle_\mathrm{e} \in [\triangle_{\mathrm{e,\,min}}, \infty\rangle$, $\triangle_{\mathrm{e,\,min}} > 0$

Assumption 4. $U_\mathrm{d} \in [U_{\mathrm{d,min}}, \infty\rangle$, $U_{\mathrm{d,min}} > 0$,

where Assumption 2 means that the path must be regularly parameterized. Then, by considering $\boldsymbol{\xi} = \left[\boldsymbol{\varepsilon}^\top, \mathbf{z}_\mathrm{g}^\top\right]^\top$, we arrive at the following proposition

Proposition 5. The equilibrium point $\boldsymbol{\xi} = \mathbf{0}$ is rendered uniformly globally asymptotically and locally exponentially stable (UGAS/ULES) under assumptions (2-4) when applying (12-13) with (10) and (27).

PROOF. Since the origin of system $\Sigma_{\mathrm{A.2}}$ is shown to be UGAS/ULES in Proposition 1, the origin of the unperturbed system $\Sigma_{\mathrm{A.1}}$ (i.e., when $\mathbf{z}_\mathrm{g} = \mathbf{0}$) is trivially shown to be UGAS/ULES by applying standard Lyapunov theory to (16) and (24), and the interconnection term satisfies $\left|\mathbf{g}_{\mathrm{A.1}}(t, \boldsymbol{\varepsilon}, \mathbf{z}_\mathrm{g})\right| = 1$, the proposed result follows directly from Theorem 7 and Lemma 8 of (Panteley *et al.* 1998).

Note that the stability result of Proposition 5 is also known as global κ-exponential stability, as defined in (Sørdalen and Egeland 1995).

2.3.2.2. Synchronization Loop Design Here, we determine the required *size* of $\boldsymbol{\alpha}_\mathrm{v}$ (i.e., U_d) such that a vessel controlled by (12) and (13) with reference signals given by (10) and (27) synchronizes with the target point. Consequently, consider

$$V_{\tilde{\varpi}} = \frac{1}{2}\tilde{\varpi}^2, \tag{31}$$

where

$$\tilde{\varpi} = \varpi_\mathrm{c} - \varpi_\mathrm{t}, \tag{32}$$

and differentiate the CLF to ultimately obtain

$$\dot{V}_{\tilde{\varpi}} = -k_{\tilde{\varpi}}\frac{\tilde{\varpi}^2}{\sqrt{\tilde{\varpi}^2 + \triangle_{\tilde{\varpi}}^2}} + \tilde{\varpi}z_\mathrm{c} \tag{33}$$

where

$$k_{\tilde{\varpi}} = \sigma\frac{U_\mathrm{t}}{|\mathbf{p}_\mathrm{t}'|}, \sigma \in \langle 0, 1] \tag{34}$$

and $z_\mathrm{c} = \dot{\varpi}_\mathrm{c} - \alpha_\mathrm{c}$. Here, α_c represents the desired speed of the collaborator when the marine craft has converged to the path, chosen as

$$\alpha_\mathrm{c} = \frac{U_\mathrm{t}}{|\mathbf{p}_\mathrm{t}'|}\left(1 - \sigma\frac{\tilde{\varpi}}{\sqrt{\tilde{\varpi}^2 + \triangle_{\tilde{\varpi}}^2}}\right) \tag{35}$$

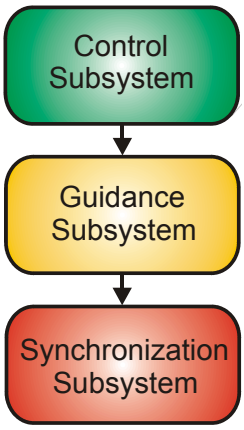

Fig. 2. The modular, cascaded nature of the motion control concept developed for DP by case A.

such that U_{d} satisfies Assumption 4 since $U_{\mathrm{d}} = \alpha_{\mathrm{c}} |\mathbf{p}_{\mathrm{c}}'|$, and where $\triangle_{\tilde{\varpi}} \in [\triangle_{\tilde{\varpi},\min}, \infty\rangle$, $\triangle_{\tilde{\varpi},\min} > 0$. Then, expand z_{c} to get

$$z_{\mathrm{c}} = \frac{U_{\mathrm{d}}(\cos\chi_{\mathrm{r}} - 1) + \gamma s}{|\mathbf{p}_{\mathrm{c}}'|} \tag{36}$$

where

$$(\cos\chi_{\mathrm{r}} - 1) = \frac{\triangle_{\mathrm{e}} - \sqrt{e^2 + \triangle_{\mathrm{e}}^2}}{\sqrt{e^2 + \triangle_{\mathrm{e}}^2}} \tag{37}$$

such that the system dynamics of $\tilde{\varpi}$ and $\boldsymbol{\xi}$ become

$$\Sigma_{\mathrm{A.3}} : \dot{\tilde{\varpi}} = f_{\mathrm{A.3}}(t, \tilde{\varpi}) + \mathbf{g}_{\mathrm{A.3}}(t, \tilde{\varpi}, \boldsymbol{\xi})^{\top} \boldsymbol{\xi} \tag{38}$$

$$\Sigma_{\mathrm{A.4}} : \dot{\boldsymbol{\xi}} = \mathbf{f}_{\mathrm{A.4}}(t, \boldsymbol{\xi}), \tag{39}$$

which is a cascaded system where the synchronization subsystem is perturbed through the well-defined

$$\mathbf{g}_{\mathrm{A.3}}(t, \tilde{\varpi}, \boldsymbol{\xi}) = \frac{1}{|\mathbf{p}_{\mathrm{c}}'|} \left[\gamma, U_{\mathrm{d}} \frac{\triangle_{\mathrm{e}} - \sqrt{e^2 + \triangle_{\mathrm{e}}^2}}{e\sqrt{e^2 + \triangle_{\mathrm{e}}^2}}, \mathbf{0}_{1\times 7} \right]^{\top}. \tag{40}$$

Note that the cascade structure is completely modular in the sense that the control subsystem ($\mathbf{z}_{\mathrm{g}}$) excites the guidance subsystem ($\boldsymbol{\varepsilon}$), which in turn excites the synchronization subsystem ($\tilde{\varpi}$), see Figure 2.

By considering the state vector $\boldsymbol{\zeta} = \left[\tilde{\varpi}, \boldsymbol{\xi}^{\top}\right]^{\top}$, we can now state the main result associated with dynamic positioning by case A through the following theorem

Theorem 6. (Case A). The equilibrium point $\boldsymbol{\zeta} = \mathbf{0}$ is rendered UGAS/ULES under assumptions (2-3) when applying (12-13) with (10) and (27) employing (35).

PROOF. Since the origin of system $\Sigma_{\mathrm{A.4}}$ is shown to be UGAS/ULES in Proposition 5, the origin of the unperturbed system $\Sigma_{\mathrm{A.3}}$ (i.e., when $\boldsymbol{\xi} = \mathbf{0}$) is trivially shown to be UGAS/ULES by applying standard Lyapunov theory to (31) and (33), and the interconnection term satisfies $|\mathbf{g}_{\mathrm{A.3}}(t, \tilde{\varpi}, \boldsymbol{\xi})| < |\mathbf{p}_{\mathrm{p}}'|_{\min}^{-1} \left(\gamma^2 + \left(\frac{U_{\mathrm{t,max}}}{\triangle_{\mathrm{e,min}}}\right)^2\right)^{1/2}$, the proposed result follows directly from Theorem 7 and Lemma 8 of (Panteley *et al.* 1998).

2.3.3. Case B: Tracking a Target Instantaneously It is not always possible, or even desirable, to design a spatial path that should be traversed. In a number of applications, the target point to be tracked is instantaneously calculated by a strategic motion planning component in the vessel DP control hierarchy. This is for instance the case in (Sørensen *et al.* 2001), where the main concern is the ability of the DP-controlled surface vessel to minimize bending stresses along a so-called marine riser, which basically is a pipe that is connected between the vessel and a point on the sea floor. Hence, we now focus on how to track a target point that is only available instantaneously, i.e., for which no future trajectory information exists. This objective encompass both point stabilization and trajectory tracking, where the former constitutes a special, degenerative case of the latter.

The suggested approach is inspired by theory from terminal missile guidance (Adler 1956), where the objective is to hit a physical target in finite time, subject to a number of real-life constraints. However, for our purposes we recognize the analogy of hitting a virtual target asymptotically, i.e., the concept of *asymptotic interception*. Specifically, we consider constant-bearing navigation by proportional navigation (PN) guidance as a suitable strategy to achieve asymptotic collision with a (virtual) target point that is to be tracked. In fact, proportional navigation is so fundamental that the claim could be made that PN is to guidance what PID is to control. The underlying guidance principle simply tries to align the relative linear velocity between the pursuer and its target along the line of sight (LOS) between them, thus achieving a collision. See Figure 3 for a simple illustration of the involved relationship. An alternative would be to align the linear velocity of the pursuer along the LOS, which is known as pure pursuit (PP) guidance, but this strategy very often results in a tail chase (equivalent to a predator chasing a prey in the animal world). In any case, if information about the linear velocity of the target is available (as is the case for our application; we decide the target motion), there is no reason why it should not be utilized to achieve PN instead of PP. In retrospect, we recognize that the guidance design of the previous section involved a type of PN guidance, where the responsibility for achieving an asymptotic intercept was shared between the vessel (pursuer) and its path-restricted collaborator (intermediate target).

We now proceed to develop the PN-associated guidance laws by Lyapunov theory. Consequently, consider the positive definite and radially unbounded CLF

$$V_{\tilde{\mathrm{p}}} = \frac{1}{2} \tilde{\mathbf{p}}^{\top} \tilde{\mathbf{p}}, \tag{41}$$

where

$$\tilde{\mathbf{p}} = \mathbf{p} - \mathbf{p}_{\mathrm{t}} \tag{42}$$

is the line-of-sight vector between the pursuer (surface vessel) and the target. Then, differentiate the CLF along the dynamics of $\tilde{\mathbf{p}}$ to obtain

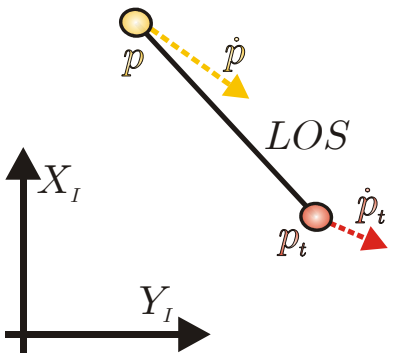

Fig. 3. The basic geometry behind tracking instantaneously. The vessel is shown in orange, while the target point is shown in red. LOS = line of sight.

$$\dot{V}_{\tilde{\mathrm{p}}} = \tilde{\mathbf{p}}^\top \dot{\tilde{\mathbf{p}}} = \tilde{\mathbf{p}}^\top (\dot{\mathbf{p}} - \dot{\mathbf{p}}_{\mathrm{t}}) = \tilde{\mathbf{p}}^\top (\mathbf{v} - \dot{\mathbf{p}}_{\mathrm{t}}) = \tilde{\mathbf{p}}^\top (\boldsymbol{\alpha}_{\mathrm{v,I}} - \dot{\mathbf{p}}_{\mathrm{t}}) + \tilde{\mathbf{p}}^\top \mathbf{z}_{\mathrm{v,I}}$$

since $\mathbf{z}_{\mathrm{v,I}} = \mathbf{v} - \boldsymbol{\alpha}_{\mathrm{v,I}}$, where $\boldsymbol{\alpha}_{\mathrm{v,I}} = \mathbf{R}_{\mathrm{B}} \boldsymbol{\alpha}_{\mathrm{v,B}}$ as in case A. Hence, by implementing PN guidance through

$$\boldsymbol{\alpha}_{\mathrm{v,I}} = \dot{\mathbf{p}}_{\mathrm{t}} - \kappa \frac{(\mathbf{p} - \mathbf{p}_{\mathrm{t}})}{|\mathbf{p} - \mathbf{p}_{\mathrm{t}}|}, \tag{43}$$

where

$$\kappa = U_{\mathrm{a}} \frac{|\mathbf{p} - \mathbf{p}_{\mathrm{t}}|}{\sqrt{\tilde{\mathbf{p}}^\top \tilde{\mathbf{p}} + \triangle_{\tilde{\mathrm{p}}}^2}} \tag{44}$$

with U_{a} representing the approach speed of the vessel toward the target (satisfying Assumption 4), and $\triangle_{\tilde{\mathrm{p}}} \in [\triangle_{\tilde{\mathrm{p}},\,\min}, \infty\rangle$, $\triangle_{\tilde{\mathrm{p}},\,\min} > 0$, we ultimately obtain

$$\dot{V}_{\tilde{\mathrm{p}}} = -U_{\mathrm{a}} \frac{\tilde{\mathbf{p}}^\top \tilde{\mathbf{p}}}{\sqrt{\tilde{\mathbf{p}}^\top \tilde{\mathbf{p}} + \triangle_{\tilde{\mathrm{p}}}^2}} + \tilde{\mathbf{p}}^\top \mathbf{R}_{\mathrm{B}} \mathbf{H} \mathbf{z}_{\nu}. \tag{45}$$

Hence, write the system dynamics of $\tilde{\mathbf{p}}$ and $\mathbf{z}_{\mathrm{g}}$ as

$$\Sigma_{\mathrm{B.1}} : \dot{\tilde{\mathbf{p}}} = \mathbf{f}_{\mathrm{B.1}}(t, \tilde{\mathbf{p}}) + \mathbf{g}_{\mathrm{B.1}}(t, \tilde{\mathbf{p}}, \mathbf{z}_{\mathrm{g}}) \mathbf{z}_{\mathrm{g}} \tag{46}$$

$$\Sigma_{\mathrm{B.2}} : \dot{\mathbf{z}}_{\mathrm{g}} = \mathbf{f}_{\mathrm{B.2}}(t, \mathbf{z}_{\mathrm{g}}), \tag{47}$$

which is a pure cascade where the control subsystem perturbs the guidance subsystem through the matrix

$$\mathbf{g}_{\mathrm{B.1}}(t, \tilde{\mathbf{p}}, \mathbf{z}_{\mathrm{g}}) = [\mathbf{0}_{2\times 1}, \mathbf{R}_{\mathrm{B}} \mathbf{H}, \mathbf{0}_{2\times 3}]. \tag{48}$$

Considering $\boldsymbol{\phi} = \left[\tilde{\mathbf{p}}^\top, \mathbf{z}_{\mathrm{g}}^\top\right]^\top$, we finally arrive at

Theorem 7. (Case B). The equilibrium point $\boldsymbol{\phi} = \mathbf{0}$ is rendered UGAS/ULES when applying (12-13) with the reference signals (10) and (43).

PROOF. Similar to that of Proposition 5.

3. CONCLUSIONS

This paper addressed the topic of dynamic positioning for fully actuated marine surface vessels. The concept of guided DP was developed by means of a modular motion control design procedure. For vessels tracking a planar target point, this work considered both the case where the target point moves along a path that is fully known in advance, as well as the case where only instantaneous information of the target point is available. A salient feature is that guided DP readily extends to underactuated vessels since it redefines the control output space to linear velocity and heading, where the heading either can be controlled independently (full actuation) or required to direct the linear velocity (underactuation). Thus, only a basic redesign of the guidance subsystem is required. For a scenario involving straight-line motion and no environmental disturbances, a redesign is unnecessary when aligning the desired heading with the desired linear velocity.

REFERENCES

Adler, F. P. (1956). Missile guidance by three-dimensional proportional navigation. *Journal of Applied Physics* **27**(5), 500–507.

Bray, D. (2003). *Dynamic Positioning*. Oilfield Publications Inc.

Breivik, M. and T. I. Fossen (2006). Motion control concepts for trajectory tracking of fully actuated ships. In: *Proceedings of the 7th IFAC MCMC, Lisbon, Portugal*.

Fossen, T. I. (2002). *Marine Control Systems: Guidance, Navigation and Control of Ships, Rigs and Underwater Vehicles*. Marine Cybernetics.

Fossen, T. I., A. Loría and A. Teel (2001). A theorem for ugas and ules of (passive) nonautonomous systems: Robust control of mechanical systems and ships. *International Journal of Robust and Nonlinear Control* **11**, 95–108.

Fossen, T. I., M. Breivik and R. Skjetne (2003). Line-of-sight path following of underactuated marine craft. In: *Proceedings of the 6th IFAC MCMC, Girona, Spain*.

Holvik, J. (1998). Basics of dynamic positioning. In: *Proceedings of the Dynamic Positioning Conference, Houston, Texas, USA*.

Panteley, E., E. Lefeber, A. Loría and H. Nijmeijer (1998). Exponential tracking of a mobile car using a cascaded approach. In: *Proceedings of the IFAC Workshop on Motion Control, Grenoble, France*.

Sørdalen, O. J. and O. Egeland (1995). Exponential stabilization of nonholonomic chained systems. *IEEE Transactions on Automatic Control* **40**(1), 35–49.

Sørensen, A. J., B. Leira, J. P. Strand and C. M. Larsen (2001). Optimal setpoint chasing in dynamic positioning of deep-water drilling and intervention vessels. *International Journal of Robust and Nonlinear Control* **11**, 1187–1205.

Sørensen, A. J., S. I. Sagatun and T. I. Fossen (1996). Design of a dynamic positioning system using model-based control. *Control Engineering Practice* **4**(3), 359–368.

Sælid, S., N. A. Jenssen and J. G. Balchen (1983). Design and analysis of a dynamic positioning system based on kalman filtering and optimal control. *IEEE Transactions on Automatic Control* **28**(3), 331–339.